

Static and dynamic calibration of radar data for hydrological use

S.J. Wood, D.A. Jones and R.J. Moore

Centre for Ecology and Hydrology, Wallingford, Oxon, OX10 8BB, UK
e-mail for corresponding author: rm@cch.ac.uk

Abstract

The HYREX dense raingauge network over the Brue catchment in Somerset, England is used to explore the accuracy of calibrated (raingauge-adjusted) weather radar data. Calibration is restricted to the use of any single gauge within the catchment so as to simulate the conditions in a typical rainfall monitoring network. Combination of a single gauge and a radar estimate is used to obtain calibrated radar estimates, with the “calibration factor” varying dynamically from one time-frame to the next. Comparing this dynamic calibration with a static (long-term) calibration factor indicates the distance from a gauge over which the dynamic calibration is useful. A tapered calibration factor is implemented which behaves in the same way as the raw dynamic calibration at short distances, tending towards the static calibration factor at larger distances. This hybrid approach outperforms raingauge, uncalibrated radar, and statically-calibrated radar estimates of rainfall for the majority of raingauges in the catchment. The results provide valuable guidance on the density of raingauge network to employ in combination with a weather radar for flood estimation and forecasting.

Keywords: radar, raingauge, calibration, rainfall, accuracy

Introduction

Accurate quantitative measurement of rainfall is a long standing problem (Rodda, 1967). A tipping-bucket raingauge provides one of the most accurate and reliable methods of rainfall measurement at a point over short time intervals, but the validity of the measurement over a large area is uncertain, particularly in convective rainfall situations. Networks of raingauges are generally employed to obtain rainfall field estimates, although the optimal design of such networks is a complex issue (Jones *et al.*, 1979; Papamichail and Metaxa, 1996). Weather radar offers significant potential advantages when spatial rainfall estimates are required: by providing a measurement over a much wider area and giving a higher resolution representation of the rainfall field structure. Radar samples a volume in space, and the intensity of the signal received is related to the number, and size, of the precipitation particles in that sample volume. Radar can provide high resolution data with a spatial scale of the order of 1 km, and 5 minutes over time, and with a spatial extent theoretically out to several hundred kilometres. However, these data may only be quantitatively useful within a radius of 75 km, particularly on account of the altitude and width of the radar beam beyond this range. To obtain similar resolution data from a network of raingauges would require a significant number of raingauges, together with significant monitoring and data quality problems (see, for example, Essery and Wilcock, 1991).

It is logical to attempt to combine the more qualitative

representation of the rainfall field distribution provided by radar, with the more quantitative point rainfall measurements made by raingauges. Such raingauge adjustment is often referred to as “radar calibration”, when the context is clear that electronic calibration of the radar is not the issue of concern. This convention is followed in the present paper. One example of raingauge calibration of radar is provided within CEH Wallingford’s HYRAD system (Moore *et al.*, 1991, 1994a, b), although there are others in operational use. The accuracy of all forms of rainfall measurement is of importance, and can have a particular bearing on the accuracy of hydrological modelling (Larson and Peck, 1974; Peck, 1980; Austin and Moore, 1996). This paper attempts to quantify the accuracy of rainfall measurement by raingauges, radar, and combinations of the two.

There are two scales of particular practical interest to hydrologists in terms of understanding rainfall variability and uncertainty. The first is for 2 km square areas, which correspond to the pixel size for which radar measurements are commonly made available. Variability, both within and across grid squares of this size, is of importance to catchment modelling, especially of the distributed type. The second is the scale of a typical catchment. In the present context this is taken to relate to the 135 km² drainage area of the River Brue gauged at Lovington (Fig. 1). Again this scale is of interest to catchment modelling, especially when using models which are lumped in form. The primary aim of this paper is to assess the accuracy with which a single raingauge and weather radar can estimate rainfall at these

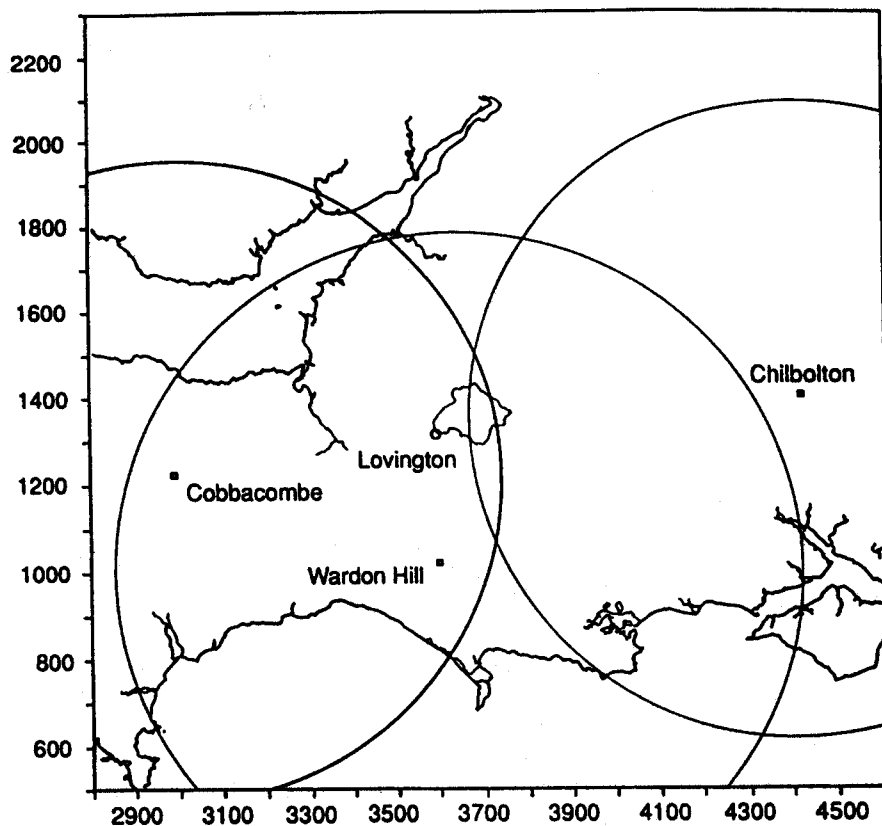


Fig. 1. The Brue catchment gauged at Lovington and the associated scanning radars (75 km radar circles indicated).

two spatial scales. Typically at this catchment scale there will be a single raingauge and access to weather radar data on a 2 km grid: the results will thus have a practical bearing on the accuracy that a hydrologist might encounter in reality.

The analysis makes use of the raingauge dataset obtained from the HYREX dense network of 49 tipping-bucket raingauges within the Brue catchment in Somerset, South-West England. This network and the associated weather radars have been described elsewhere (Wood *et al.*, 2000). Data from the Wardon Hill radar (Fig. 1) have been used exclusively because this radar provides a good example of a C-band operational radar located at a reasonable range from the catchment (circa 40 km). Features of the raingauge network of importance here are (i) two super-dense networks each with 8 gauges within a 2 km square defined by the radar grid, located in areas of high and low relief, and (ii) catchment-wide coverage with usually at least one gauge within each 2 km square. These provide the basis for obtaining high accuracy areal estimates for the two super-dense network 2 km squares and for the catchment respectively.

The main thrust of the analysis is firstly to use data from the dense raingauge network to derive accurate estimates of the mean areal rainfall over 2 km pixels and over the catchment. These "best estimates" are then used to assess how accurately they can be estimated by any single raingauge

within the catchment, by radar and by combinations of the two. Only quality-controlled raingauge values were used in forming the averages. The accuracy of these estimates has been estimated to be around 11.5% for rainfall rates of 4 mm h^{-1} (Wood *et al.*, 2000). In calculating the areal average rainfalls for the catchment a weighted average procedure was employed. Results have been obtained for a 15 minute time interval, commonly used for hydrological forecasting in the UK. This is in contrast to previous analyses which have tended to concentrate on longer time-scales such as hourly (Collier, 1986) and three hourly (Harold *et al.*, 1974) in an attempt to avoid discretisation errors. By investigating the dependence of rainfall measurement accuracy on rainfall intensity, and concentrating on the higher rainfall events, the adverse effects of discretisation can be reduced. The paper addresses the issue of the radar data calibration using measurements from each raingauge in the network in isolation. Both long-term "static" and short-term "dynamic" calibration methods are investigated and their performances compared.

Measurement of rainfall by a single raingauge

Wood *et al.* (2000) describe a simple empirical approach for

investigating how the accuracy of a rainfall estimate varies with the amount of rainfall being estimated. In the case of a 2 km pixel, the “ground truth” or “best estimate”, T , is defined as the mean of the available raingauges within it (nominally 8 raingauges). This quantity is deemed invalid if fewer than 6 of the raingauges are working satisfactorily for a given time-frame. The essence of the approach is the assumption that there are so many raingauges used in calculating T that it is essentially the same as the unknown true rainfall for the pixel. The value from each single raingauge, R , is used to define an estimate of the mean square error of R as an estimate of the true rainfall for the 15 minute time-frame, given by

$$S^2 = (R - T)^2. \quad (1)$$

The procedure involves either (i) averaging values of S^2 across time-frames or (ii) using many time-frames to construct scatter plots of $\log S$ against $\log T$ and constructing a smoothed curve through the points. Separate analyses have been done for both the high and the low relief pixels. The question arises of whether to include in T the raingauges included in the estimator R under test. The analysis was done both ways and the effect was found to be sufficiently small to be ignored.

Figure 2 shows S versus T (on logarithmic scales) for raingauge 23 sited at Milton Wood Corn Field (see Fig. 1 of Wood *et al.*, 2000), when T is the 2 km pixel rainfall at the low relief grid square. Raingauge 23 is chosen as a gauge located near the centre of the catchment; it is about 3 km from the 2 km low relief square. A distinction is made in Fig. 2 between convective and frontal type rainfall. The quantity S is seen to increase as T increases, with the

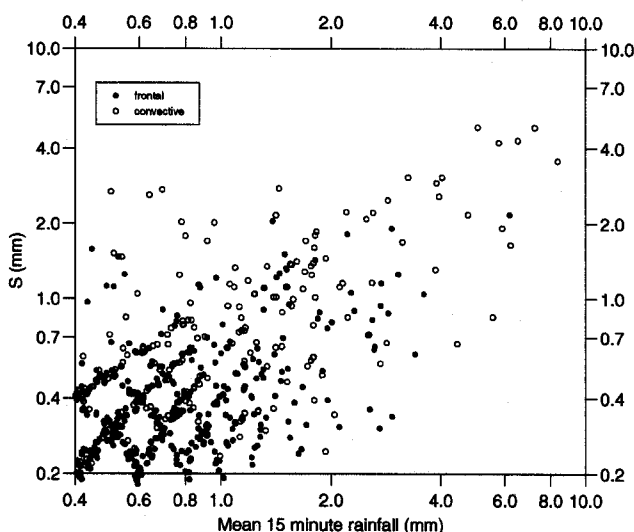


Fig. 2. Standard error of rainfall estimate based on raingauge 23 (Milton Wood Corn Field), S , as an estimate of the 2 km pixel rainfall over the low relief grid square, T . Convective and frontal type rainfall are distinguished as shown.

convective events dominating the higher values of T . There is also evidence of the effects of discretisation for lower values of T .

The RMS (root mean square) error, S , in estimating the low relief 2 km pixel rainfall was calculated at each of the raingauge sites *within the catchment* and plotted in Fig. 3 against distance of the gauge from the pixel. Two categories of rainfall intensity are distinguished. Medium-intensity rain was taken to include all 15 minute periods with rainfall amounts in the range 1–3 mm, corresponding to rainfall intensities of 4–12 mm h⁻¹. High-intensity rain was defined as 15 minute periods with rainfall in the range 3–10 mm, corresponding to rainfall intensities of 12–40 mm h⁻¹. Note that since the ground truth estimate is for a 2 km pixel area, formed as the average of gauge values in it, the values cover a smaller range than do those occurring at a single raingauge. For both medium and high rainfall categories, Fig. 3 shows the RMS error increases for raingauges further away from the pixel, with the effect being more pronounced in the case of heavy rain. Similar behaviour was obtained when using the high relief grid square as the basis of the analysis. The greater increase in error with distance for high-intensity rainfalls is probably due to more convective rainfall being included, showing variability over smaller spatial scales.

Measurement of rainfall by radar

The UK network of operational radars operate at C-band, with an approximate wavelength of 5 cm, and they rotate to map out snapshots of the rainfall field at a series of elevations. Cartesian grids of rainfall values (mm h⁻¹) are

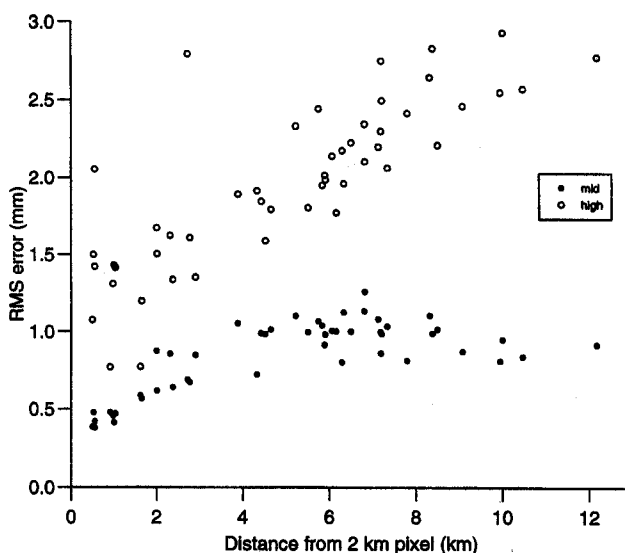


Fig. 3. RMS error of rainfall estimate from a single gauge within the catchment, S , in measuring the low relief 2 km pixel rainfall, T . Medium and high rainfall categories are distinguished as shown.

derived from the polar radar reflectivity values using a suite of algorithms (Collier and James, 1986). These rainfall grid values are produced every 5 minutes on both a 2 km and 5 km grid. Data from the lowest beam are used routinely for hydrological applications, and these are usually mixed with data from the next highest beam in an "infill area" where the lowest beam is affected by blockages. For this study, radar and raingauge rainfalls are compared by identifying the coincident grid square and calculating R_r , the 15 minute radar rainfall total in mm between time $t-15$ and time t , as the weighted average

$$\frac{R_t + 2R_{t-5} + 2R_{t-10} + R_{t-15}}{24} \quad (2)$$

where R_{t-i} is the radar rainfall intensity in mm h^{-1} at time $t-i$ minutes. The 15 minute radar rainfall total is undefined if any of the 4 rainfall rates in the 15 minute interval are themselves undefined.

Thirty months of 15 minute rainfall data, from January 1994, were analysed. No quality control measures were carried out on the radar data of the kind applied to raingauge data (Wood *et al.*, 2000). However, comparisons between radar and raingauge data did reveal the existence of some periods of anomalous propagation. These were not formally identified since they coincide with periods of zero observations at the raingauges which are automatically separated out by the analysis. Snowfall events were identified from Meteorological Daily Weather Summaries and removed from the analysis. The accuracy of radar in measuring snowfall is not of concern here; Collier and Larke (1978) provide a discussion of this problem in a UK context.

To investigate the dependence of radar rainfall accuracy on rainfall intensity, scatter plots of S versus T were created similar to Fig. 2. However, now R is the radar value whilst T is again the average of the 8 raingauges contained within the low relief 2 km pixel. Scatter plots of S versus T were obtained for the 2 km and 5 km resolution data and Fig. 4 shows them displayed as a smoothed line fitted to the scatter of points, following the procedure described by Wood *et al.* (2000). Figure 4 also shows how the radar rainfall estimate compares in accuracy with the single-gauge (within pixel) estimate for rainfall over the low relief 2 km grid square. As expected the 2 km data are seen to provide a more accurate estimate than the 5 km data, although the difference is marginal except for the high rainfall amounts (>2 mm). The accuracy of the raingauge estimate is seen to be consistently better than radar across the full range of rainfall values.

When comparing raingauge and radar performance within the catchment, interest is usually centred on using the value for a distant raingauge as an estimate of rainfall in a given pixel. In contrast, when radar estimates are concerned there is no need to rely on the value for a remote radar pixel since a coincident radar value at the point of interest will be available. This idea reinforces the advantages of radar in providing measurements over a very wide area. Two important questions lead on from this, however. Firstly, at

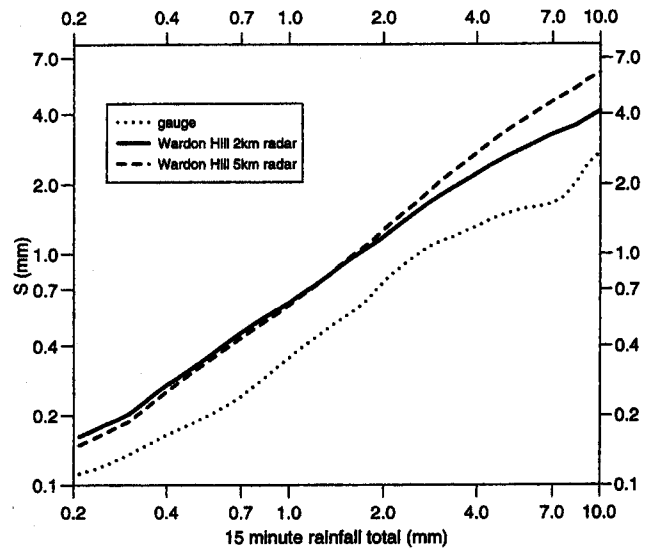


Fig. 4. Standard error of a single gauge and 2 km and 5 km radar data, S , as estimates of the low relief 2 km pixel rainfall, T .

what distance from a 2 km pixel will the raingauge measurement become so unrepresentative that it is outperformed by the coincident radar pixel? And secondly, to what extent can raingauge calibration of the coincident radar pixel value improve its accuracy even more? The analyses below attempt to address these two questions.

Values for the catchment average rainfall were calculated from raingauge values using the weighted average procedure outlined in Wood *et al.* (2000). This forms an average within each 2 km pixel containing a raingauge and these in turn are averaged to obtain a catchment average value. Corresponding radar estimates of catchment average rainfall, for both 2 km and 5 km resolution data, were calculated as area-weighted averages of the radar values for pixels contained, wholly or partly, within the catchment boundary. The quantity S , defined as the root mean square error of the radar estimate of the areal rainfall rate, is again defined by Eqn. (1). Figure 5 presents the smoothed line fitted through the scatter of S versus T values, obtained using Wardon Hill radar data on a 2 km and 5 km grid for a 15 minute time interval. It also shows how the accuracy of the radar compares with that of any single raingauge, on average, in estimating the catchment average rainfall for a 15 minute time interval. Note that the accuracy of the single raingauge estimate is slightly worse than obtained using radar, across the full range of rainfall values. Comparison of Figs. 4 and 5 shows that the accuracy of radar estimates is relatively unaffected by the change from a 2 by 2 km target to the catchment scale, while the accuracy of the single raingauge estimate deteriorates markedly.

When considering the causes of error in radar rainfall measurement it is important to be aware of the configuration of the radar installation with regard to location, hardware specification, and other factors. The Wardon Hill radar is

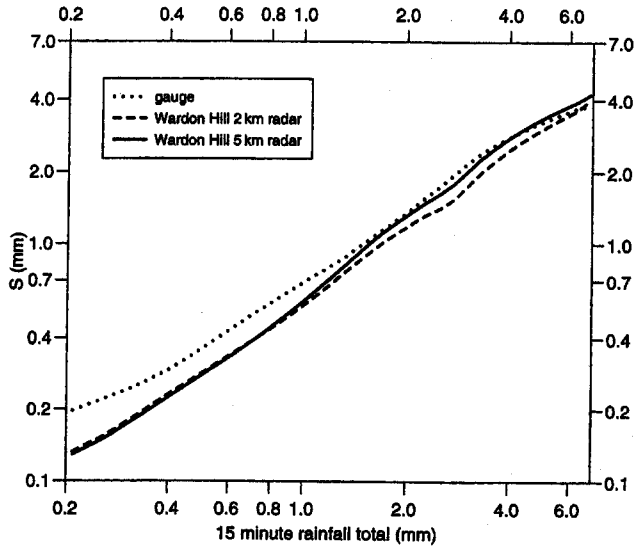


Fig. 5. Standard error of a single gauge and 2 km and 5 km radar data, S , as estimates of the catchment average rainfall, T .

situated about 40 km south of the Brue catchment at National Grid Reference 3609 1023 and at an elevation of 255m AMSL. At this range the lowest radar beam (0.5°) is at a height of approximately 0.4 km above the ground. Some of the major factors affecting radar rainfall accuracy are Bright Band, orographic enhancement, attenuation, and anomalous propagation, as well as hardware fluctuations in the actual radar performance. Collier (1996) and Joss and Waldvogel (1990) provide recent reviews. An attenuation correction is included in the radar data processing but, despite this, all five of the factors can be assumed to be affecting, to varying degrees, the radar data analysed here. No attempt has been made here to correct further the radar data. Since the analyses have focussed on examining the accuracy of rainfall as a function of rainfall intensity, the error of measurement when the actual rainfall is zero has largely been excluded. This includes many cases of anomalous propagation, an effect which gives rise to spurious radar rainfall echoes in anticyclonic conditions due to the radar beam being bent towards the ground.

Measurement of rainfall by raingauge-calibrated radar

INTRODUCTION

A rainfall field, varying over space and evolving in time, can be an extremely complex structure. That structure can be measured by raingauges or weather radar. Whilst raingauges provide reasonably accurate measurements of point rainfall near the ground, a considerable number of raingauges would be required to obtain a representation of the rainfall field structure, and this would prove prohibitively expen-

sive. By contrast, weather radar produces a representation of the structure of the rainfall field, but the quantitative measurements are less accurate than can be obtained by raingauges. By combining the two measurement methods there is the prospect of a more accurate representation of the rainfall field, both in qualitative and quantitative terms.

A number of options exists for combining radar and raingauge data to obtain improved rainfall field estimates (Moore, 1990). These range from space-time models of the rainfall field, which incorporate the covariance structure of the rainfall field and measurement errors, to simpler formulations based on optimal linear interpolation (Jones *et al.*, 1979), Kriging (Creutin and Obled, 1982) or surface fitting (Moore *et al.*, 1994a). All these methods will involve, at some level, the use of a raingauge calibration factor. Typically this will be some form of ratio of raingauge and coincident radar values. In a typical catchment containing 1 or 2 raingauges such a calibration factor can be calculated for a particular region and then applied more widely to correct the entire radar image. Two basic categories of calibration factor are investigated here: long-term mean (static) factors and short-term (dynamic) factors. Long-term calibration factors involve the calculation of a single corrective term from a historical dataset, which is subsequently applied to all time frames in an identical way. In contrast, the "dynamic" calibration factor is recalculated every 15 minutes. A hybrid method which tapers off the effect of the raw dynamic calibration factor at large distances is also investigated. The partitioning of the calibration factor into spatially-uniform long-term and spatially-varying dynamic components contrasts with recent real-time recursive estimation schemes for mean field bias correction which have no spatially varying component (Smith and Krajewski, 1991; Seo *et al.*, 1999).

STATIC CALIBRATION FACTORS

There is a wide variety of options for defining the long-term bias of a radar dataset. Two types of long-term calibration factor were examined as a means of characterising bias, and potentially correcting for it. The first type considered is the long-term arithmetic mean ratio bias calculated over n time-frames from

$$B = \frac{1}{n} \sum \frac{R_g}{R_r} \quad (3)$$

and the second is the geometric mean ratio bias

$$B = \left(\prod \frac{R_g}{R_r} \right)^{\frac{1}{n}} \quad (4)$$

Here, R_g and R_r denote the 15 minute raingauge and radar rainfall values (in mm) respectively. A lower threshold of 0.2 mm for R_g is imposed to minimise discretisation errors and the influence of anomalous propagation; the same threshold is used for R_r to ensure the ratio is defined.

Using the 2 km resolution radar data, the values of these

Table 1. Raw static calibration factors calculated at 49 rain-gauge sites within the Brue catchment. Summary statistics indicate the variation between rain-gauge sites.

	Arithmetic Mean	Geometric Mean
Minimum value	1.16	1.19
Maximum value	1.70	1.65
Average value	1.34	1.37
Standard deviation	0.15	0.12

two bias measures, or calibration factors, were evaluated for each of the 49 rain-gauges in the catchment using 30 months of continuous data from January 1994. The results are summarised in Table 1. The mean value for the two types of calibration factor are seen to be very similar and the arithmetic mean bias is used to obtain subsequent results. In both cases the range of calculated values was seen to be quite large and the higher values related well to areas of high relief in the catchment. This variability is important since the results from any particular rain-gauge site could be chosen, operationally, to define a static radar calibration factor. Applying each of these calibration factors in turn will give an indication of how much a change in the calibration factor value would affect radar accuracy. The measured radar values over the low relief grid square have been calibrated in this way, using the calibration factor derived for each gauge in turn. Figure 6 shows the resulting RMS errors of the calibrated 2 km radar data plotted against each of the 49

rain-gauges used to provide the static calibration factor. Results are shown for the two categories of rainfall defined earlier as medium (4–12 mm h⁻¹) and heavy (12–40 mm h⁻¹) rainfall. The two near constant lines show the RMS error for the *uncalibrated* radar data in the two categories. It is seen that a range of improvements is available by using the range of static calibration factors calculated using these methods. For the heavier rainfall events it appears that the static calibration offers a significant improvement over the uncalibrated radar with an average improvement of around 40%, reducing the RMS error from 2.4 to 1.5 mm. The 4–12 mm h⁻¹ category rainfall is, on the other hand, not really improved and in most cases the RMS error is seen to actually increase. There is an element of sampling bias in these conclusions since (i) when the “true” rainfall is high a typical radar value will require a large calibration factor applied to it to reproduce the high observation, whereas (ii) if the “true” value is only moderate, applying the same calibration factor will produce a worse result than the raw estimate. Nevertheless, the categorisation into medium and high intensity rainfall periods is retained since it provides a useful basis for comparing different methods for dynamic calibration.

For later purposes a fixed static calibration factor of 1.35 is used for all locations. For medium rainfall this gave RMS errors of 0.95 mm when averaged across the gauges, compared with 0.8 mm for the uncalibrated radar. For high rainfall the corresponding values are 1.8 and 2.4 mm. This calibration factor is clearly derived from an analysis of the whole dataset. In practice, calibration factors must be determined from data before, and possibly including, the

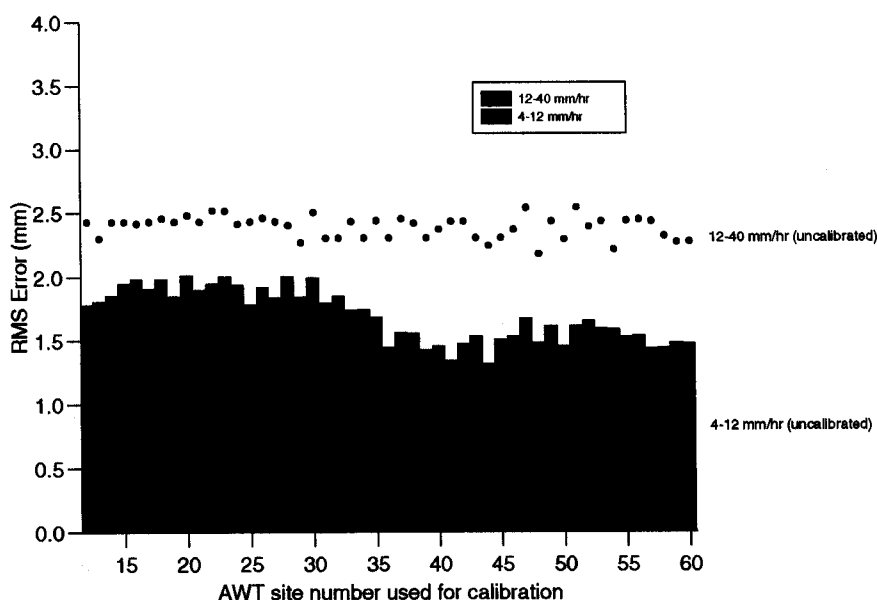


Fig. 6. RMS error over the low relief pixel of the calibrated 2 km radar data for each of the 49 rain-gauges used for climatological calibration. The errors for medium and heavy rain are distinguished as indicated. The two near constant lines show the error for the uncalibrated radar data for these two categories.

time-point at which rainfall estimation is being applied. The procedure used here for setting the static calibration factor departs from this ideal. Little variation in the calibration factor over time was found, suggesting that a “good” calibration factor can be determined from a short amount of data. The sensitivity study illustrated by Fig. 6 shows that the assessment would be little affected if the calibration factor were changed by quite a large amount.

DYNAMIC CALIBRATION

It has been shown that the spatial variability of both types of calibration factor – the arithmetic mean ratio bias and the geometric mean ratio bias – is significant. This leads logically to the use of a calibration “map” where a field of calibration factors is calculated and applied to the radar field, pixel by pixel. Of course, this implies the need for further raingauges so that an acceptable representation of the rainfall field can be used to recalibrate the radar data.

Additionally, the use of long-term ratios might be improved upon by employing “dynamic” calibration factors. Application of dynamic calibration fields calculated in near real-time is the basis of CEH Wallingford’s HYRAD system (Moore *et al.*, 1994a, b). The basis of the method is to fit a mathematical surface to calibration factor values calculated at a number of raingauge locations and to scale the radar rainfall field by the coincident factor values to derive a more accurate calibrated radar field. For the present purposes, where only one gauge is to be used for calibration, a more direct approach is appropriate which is developed below.

Attention is centred, in these assessments, on the case where the timeliness of data availability is such that a set of calibration factors determined in a given time-frame can be applied to the same time-frame. This is possible in typical UK applications in the case where 15-minute totals are the radar data of interest, since telemetered raingauge information is acquired at this resolution. However, the most up-to-date radar data would be received at a 5 minute interval and, if these data were to be calibrated using available raingauge data, there would need to be some projection in time of the calibration factors. This situation has not been addressed in this study.

Various dynamic calibration factors were tried and the most satisfactory choice found to be that defined, for a given gauge, by

$$c = \frac{R_g + \varepsilon}{\kappa R_r + \varepsilon} \quad (5)$$

where R_g and R_r are the raingauge and coincident radar grid-square values in mm for a 15 minute interval. The parameter ε is a positive value which ensures that the calibration factor is defined for radar values equal to zero, and κ is the long-term static calibration factor; both parameters are fixed across all gauges. Once the dynamic

calibration factor is calculated, the calibrated radar value R^* is calculated from the expression

$$R^* = c(\kappa R_r + \varepsilon) - \varepsilon \quad (6)$$

where R_r is now the radar value for the target pixel. This method of dynamic calibration was adopted for the present study for reasons of computational efficiency, directness of approach and simplicity. The HYRAD system makes use of many raingauges for calibration and uses a surface fitting technique applied to the calibration factors to calculate the value c for a given pixel. Here the appropriate c is found by a more direct transfer: in the simplest case, the single value, c , calculated for the pixel containing the raingauge, is applied to all radar pixels. Note that the definition of the calibration factor in Eqn. (5) is such that a value is obtainable under all conditions and there is no need for a special treatment when either the radar-pixel or the gauge indicates zero rainfall. The initial version of the HYRAD calibration procedure uses a slightly different form of Eqn. (5) for its calibration factor, with a corresponding change to Eqn. (6), in which the static factor κ is omitted ($\kappa = 1$), and in which two different values of ε are used in the numerator and denominator, both of which were treated as values to be fixed by various performance comparisons. It now seems better to use the form in Eqn. (5) since one of the adjustable parameters can be determined from the study of long-term bias in the radar data, which is worthwhile on its own merits.

The value of ε is crucial to the performance of the dynamic calibration method; a very large value will cause the calibration factor c to approximate to unity thus offering no change from the original radar value, whilst a very small value will make the factor oversensitive and take on an unrealistic range of values. A range of values for ε was tested and a value of unity was generally seen to offer quite stable results for raingauges close to the 2 km pixel whose rainfall estimate is required. Figures 7a and 7b show the impact of a dynamic calibration with $\varepsilon = 1$ mm when each raingauge in turn is used as the calibrating raingauge for estimating rainfall over the low relief pixel. The plots show RMS error of the dynamically calibrated radar data, for the medium and heavy rainfall categories defined earlier, as a function of raingauge distance from the area of calibration. It appears that the dynamic calibration performs quite erratically. At distances close to the low relief grid square the performance is as good as that of a single raingauge, and is better than both the radar grid-square and the statically calibrated radar estimates. At distances on the far side of the catchment the performance is again good and outperforms the raingauge as well as the uncalibrated and statically calibrated radar. However, there is a range of distances over which the performance appears worse than even the uncalibrated radar data. This is true for both the medium and heavy rainfall categories although larger increases in RMS error are seen to be introduced into the medium-sized rainfall when the dynamic calibration is used. The performances of the

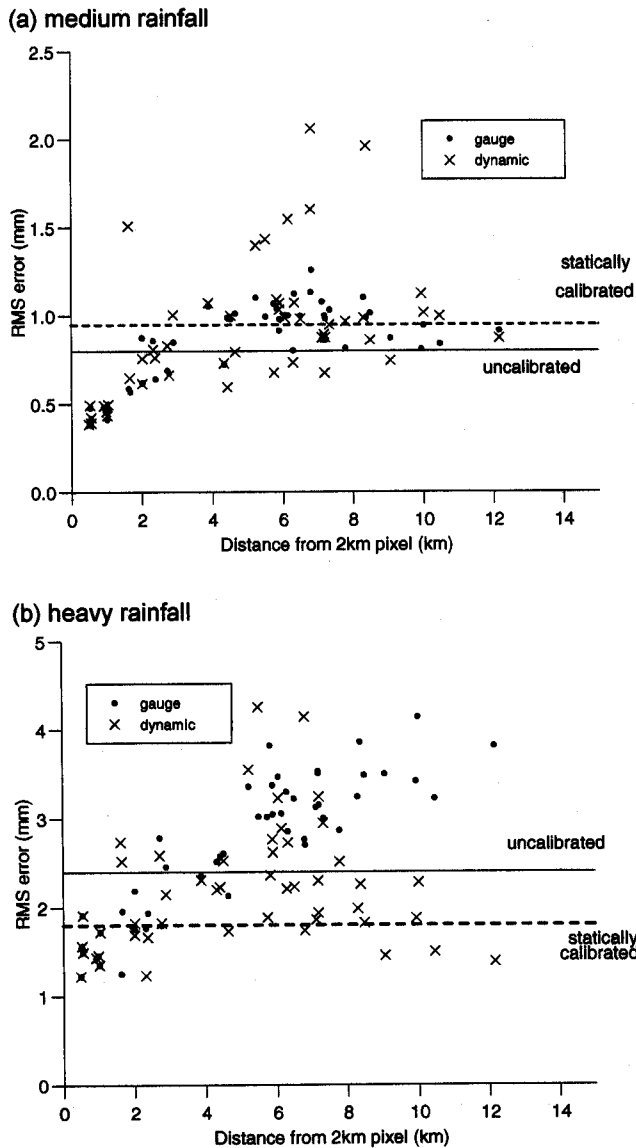


Fig. 7. RMS error over the low relief pixel of the dynamically calibrated radar data and of a single gauge, for the medium and heavy rainfall categories, as a function of raingauge distance from the area of calibration. The error of the uncalibrated radar data is also shown.

uncalibrated and statically calibrated radar are shown as horizontal lines. These are actually each single values for the estimation accuracy of the radar value for the target pixel itself, rather than using a radar pixel value elsewhere to estimate the target.

TAPERED DYNAMIC CALIBRATION

One solution to the erratic performance of the dynamic calibration approach is to introduce a tapered dynamic calibration factor which will take on the form of the dynamic calibration at short distances but behave like the static calibration at long distances. A proposed form of this

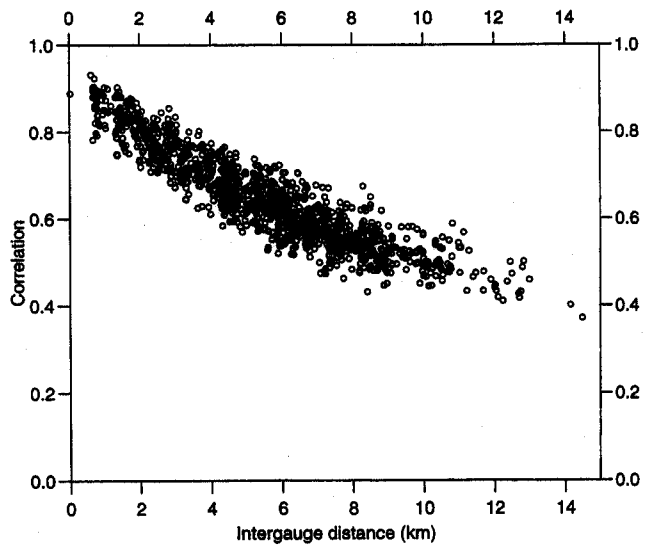


Fig. 8. Spatial correlation function of the dynamic calibration factor.

calibration factor is

$$c^* = 1 + \rho(c - 1) \tag{7}$$

where ρ is essentially the spatial correlation function of c , defined as a function of distance from the radar pixel to be calibrated. Equation (7) has that obvious derivation that the formula provides the optimal approximation to a random surface whose mean value is 1, which has the correlation function ρ and for which a single observation, c , is available. The sample estimate for ρ is shown in Fig. 8 and this was approximated by an exponential function for this calibration procedure. (Note that there is a pair of raingauges at a very close distance within the overall network, which provides the correlation value for a small distance.) In turn, a revised expression for the calibrated radar estimate is defined as

$$R^* = (1 + \rho(c - 1))(\kappa R_r + \varepsilon) - \varepsilon \tag{8}$$

which reduces to the dynamic calibration of Eqn. (6) when $\rho = 1$ and to the static calibration, $R^* = \kappa R_r$, when $\rho = 0$. The effect of this calibration factor on the 2 km radar data in the medium and heavy defined rainfall categories is shown in Fig. 9. For the 12–40 mm h⁻¹ category the tapered calibration factor approach is seen to outperform raingauge, uncalibrated radar, and average statically calibrated radar for the entire range of intergauge distances. This is not however true of the 4–12 mm h⁻¹ category where the tapered calibration method performs similarly to use of a single raingauge, although there is the suggestion of some improvement over the range 4 to 8 km. A comparison of these two categories of rainfall should bear in mind the biasing effects of the categorisation noted previously with reference to static calibration factors. Taking this into account there appears to be reasonable evidence that the tapered dynamic calibration procedure performs as well as

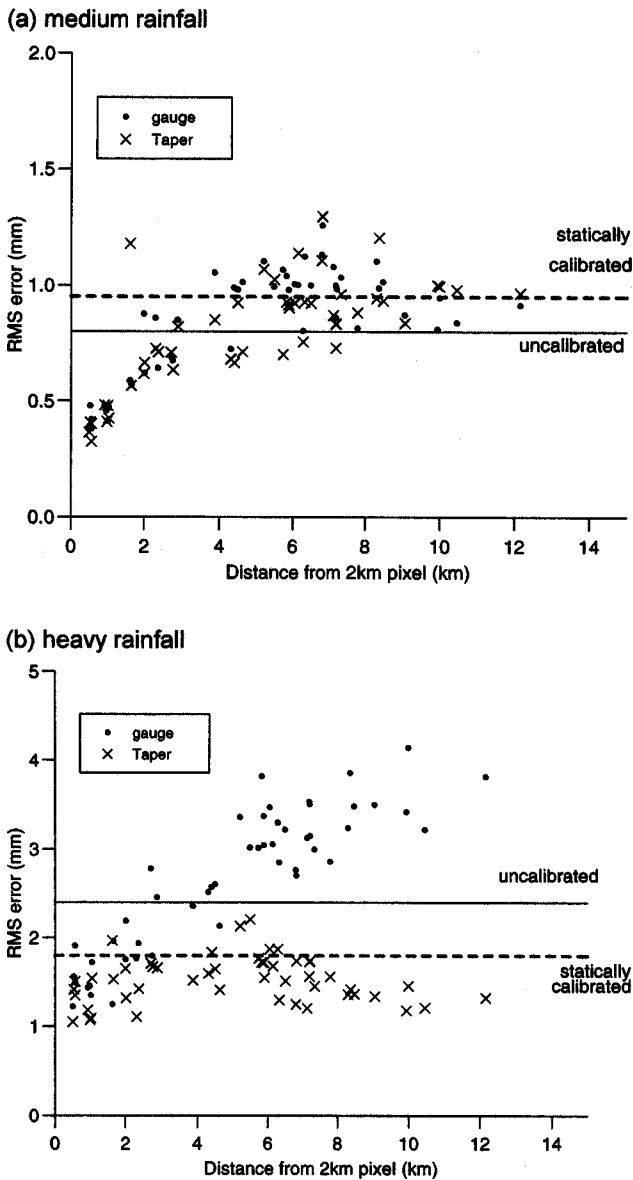


Fig. 9. RMS error over the low relief pixel of the tapered calibrated radar data and of a single gauge, for the medium and heavy rainfall categories, as a function of raingauge distance from the area of calibration. The error of the uncalibrated radar data is also shown.

the better of uncalibrated radar or raingauge estimates of rainfall.

It is notable from Fig. 7 that use of a single raingauge to estimate rainfall, without the benefit of radar data, is only better than using radar for up to 3–4 km from the gauge. This is a reflection of the spatial variability of rainfall on a 15-minute timescale. Figure 9 indicates that, at least for high rainfall intensities, a combination of the gauge value with radar data using the distance-tapered form of the calibration factor can lead to an improvement over just using the radar data, even if it is given a static calibration adjustment, out to distances of at least 14 km, the largest distance studied.

Conclusions

Thirty months of raingauge data at a 15 minute time-scale have been analysed with the main aim of quantifying the accuracy with which rainfall can be measured by a raingauge, by radar and a combination of the two. An empirical approach has been pursued in which scatter plots of mean rainfall and estimation accuracy were used to define a relation between these. RMS error has been calculated for two categories of rainfall: medium-rainfall of intensity 4–12 mm h⁻¹ and heavy-rainfall of intensity 12–40 mm h⁻¹ averaged over a 2 km pixel.

Two superdense networks, having 8 gauges within a 2 km grid square area, were used to obtain the “best estimate” or “ground truth” rainfalls for these squares. The accuracy of individual raingauges in estimating the mean grid-square rainfall was found to worsen as the distance from the grid-square centre increased. The performance of a single gauge, in general, in estimating the catchment average rainfall was seen to be much worse than a gauge measuring the rainfall over a single 2 km grid square. This intuitively reasonable result simply confirms that there are limits to how far the measurements from a single gauge can be extrapolated usefully in space.

Radar estimates of rainfall, using both 2 and 5 km resolution data, were analysed. When used as estimates of the 2 km pixel rainfall it was found that the 2 km radar data were more accurate than the 5 km data, as expected, but neither could match the accuracy of using a “typical” single gauge located within the 2 km pixel. It was found that a gauge is only better than radar at estimating 2 km pixel rainfall if the gauge is within 3 to 4 km of the pixel centre. When estimating the catchment average rainfall, it was again seen that the 2 km radar data outperformed the 5 km resolution data but, in this case, both resolutions of radar data outperformed a typical gauge estimate. This is, of course, not entirely unexpected since a radar can provide field estimates at a better spatial resolution than the constant value derived from the point gauge measurement. However, radar suffers from worse accuracy than a raingauge at a point.

The accuracy of raingauge and radar used in combination was considered as a problem of raingauge adjustment, referred to here as “radar calibration”, noting that electronic hardware calibration of the radar is not the issue in question. Long-term bias statistics were calculated at each of the gauge sites in the catchment to derive an ensemble of long-term static calibration factors. These had an average value of around 1.3, indicating under-estimation by radar, but varied in size across the catchment from as little as 1.1 up to around 1.6. This range of static calibration factors was applied to the radar values to investigate sensitivity to this factor. Next, a generalised dynamic calibration factor was implemented with a damping term, ϵ , which allows cases with zero radar or raingauge values to be calibrated. Initial studies showed

that this form of calibration factor behaved rather erratically with a good performance close to the gauge being used for calibration but degrading at distances of more than 5 km away. This led to the introduction of a tapered form of calibration factor which behaves as a dynamic calibration factor at short distances but reduces to a static calibration factor at larger distances. The initial results are promising, particularly for high rainfall amounts. For multiple gauge networks, these results suggest that an improved operational radar calibration procedure will be obtained by performing an initial static adjustment to the radar field and that there should be further investigation of dynamic calibration procedures. This would potentially provide improvements to the capabilities of existing operational procedures such as the HYRAD system.

References

- Austin, R.M. and Moore, R.J., 1996. Evaluation of radar rainfall forecasts in real-time flood forecasting models. *Quaderni Di Idronomia Montana*, 16, 19–28.
- Collier, C.G., 1986. Accuracy of rainfall estimates by radar, Part II: comparison with raingauge network. *J. Hydrol.*, 83, 225–235.
- Collier, C.G., 1996. *Applications of Weather Radar Systems: A Guide to Uses of Radar Data in Meteorology and Hydrology*. Wiley, Chichester, UK, Second Edition, 390 pp.
- Collier, C.G. and James, P.K., 1986. On the development of an integrated weather radar data processing system. *23rd Conference on Radar Meteorology*, 22–26 September, Snowmass, Colorado, 95–98.
- Collier, C.G. and Larke, P.R., 1978. A case study of the measurement of snowfall by radar: an assessment of accuracy. *Quart. J. Roy. Meteorol. Soc.*, 104, 615–621.
- Creutin, J.D. and Obled, C., 1982. Objective analysis and mapping techniques for rainfall fields: an objective comparison. *Water Resour. Res.*, 18, 413–431.
- Essery, C.I. and Wilcock, D.N., 1991. The variation in rainfall catch from standard UK Meteorological Office raingauges: a twelve year case study. *Hydrol. Sci. J.*, 36, 23–34.
- Harold, T.W., English, E.J. and Nicholass, C.A., 1974. The accuracy of radar-derived rainfall measurements in hilly terrain. *Quart. J. Roy. Meteorol. Soc.*, 109, 589–608.
- Jones, D.A., Gurney, R.J. and O'Connell, P.E., 1979. Network design using optimal estimation procedures. *Water Resour. Res.*, 15, 1801–1812.
- Joss, J. and Waldvogel, A., 1990. Precipitation measurement and hydrology. In: *Radar in Meteorology*, D. Atlas (Ed.), Battan Memorial and 40th Anniversary Radar Meteorology Conference, Chapter 29a, American Met. Soc., 577–606.
- Larson, L.W. and Peck, E.L., 1974. Accuracy of precipitation measurements for hydrologic modeling. *Water Resour. Res.*, 10, 857–863.
- Moore, R.J., 1990. Using meteorological information and products. In: *Use of meteorological data and information in hydrological forecasting*, A. Price-Budgen (Ed.), 377–396, Ellis Horwood, Chichester, UK.
- Moore, R.J., Watson, B.C., Jones, D.A. and Black, K.B., 1991. Local recalibration of weather radar. In: *Hydrological Applications of Weather Radar*, I.D. Cluckie and C.G. Collier (Eds.), 65–73, Ellis Horwood, Chichester, UK.
- Moore, R.J., May, B.C., Jones, D.A. and Black, K.B., 1994a. Local calibration of weather radar over London. In: *Advances in Radar Hydrology*, M.E. Almeida-Teixeira, R. Fantechi, R. Moore and V.M. Silva (Eds.). Proc. Int. Workshop, Lisbon, Portugal, 11–13 November 1991, Report EUR 14334 EN, European Commission, 186–195.
- Moore, R.J., Jones, D.A., Black, K.B., Austin, R.M., Carrington, D.S., Tinnion, M. and Akhondi, A., 1994b. RFFS and HYRAD: Integrated systems for rainfall and river flow forecasting in real-time and their application in Yorkshire. "Analytical techniques for the development and operations planning of water resource and supply systems, BHS National Meeting, University of Newcastle, 16 November 1994, *BHS Occasional Paper No. 4*, British Hydrological Society, 12 pp.
- Papamichail, D.M. and Metaxa, I.G., 1996. Geostatistical analysis of spatial variability of rainfall and optimal design of a rain gauge network. *Water Resour. Management*, 10, 107–127.
- Peck, E.L., 1980. Design of precipitation networks. *Bull. Am. Meteorol. Soc.*, 61, 894–902.
- Rodda, J., 1967. The systematic error in rainfall measurement. *J. Inst. Water Engng.*, 21, 173–177.
- Seo, D.-J., Breidenbach, J.P. and Johnson, E.R., 1999. Real-time estimation of mean field bias in radar rainfall data. *J. Hydrol.*, 223, 131–147.
- Smith, J.A. and Krajewski, W.F., 1991. Estimation of the mean field bias of radar rainfall estimates. *J. Appl. Meteorol.*, 30, 397–412.
- Wood, S.J., Jones, D.A. and Moore, R.J., 2000. Accuracy of rainfall measurement for scales of hydrological interest. *Hydrol. Earth System Sci.*, 4, 531–543.